ANALYSIS AND PREDICTION OF SPACE ENVIRONMENTALLY INDUCED SPACECRAFT ANOMALIES

J.-G. Wu[1,2], H. Lundstedt[2], L. Eliasson[3], A. Hilgers[4]

[1] Solar-Terrestrial Physics Division, Danish Meteorological Institute
Lyngbyvej 100, DK-2100 Copenhagen, Denmark
[2]Solar-Terrestrial Physics Division, Swedish Institute of Space Physics
Box 43, S-221 00 Lund, Sweden
[3]Swedish Institute of Space Physics, Box 812, S-981 28 Kiruna, Sweden
[4]ESTEC, European Space Agency, Noordwijk, NL-2200 AG, The Netherlands

ABSTRACT

We investigate how the two geostationary spacecraft, ESA Meteosat-3 and Swedish Tele-X, are affected by space weather (characterised by daily-averaged Dst, daily sum of Kp, and daily-averaged energetic electron flux (> 2 MeV)) through superposed epoch analysis and develop neural network models to predict spacecraft anomalies one day in advance. From superposed epoch analysis we find (1) that the spacecraft anomalies frequently occurred during the recovery phase of geomagnetic storms; (2) that the space environment during the last 4-6 days preceding an anomaly contributes statistically the most to the anomaly occurrence; (3) that Kp and Dst would be better parameters than the energetic electron flux (> 2 MeV) to predict anomalies on Meteosat-3, implying that the anomalies on Meteosat-3 were mainly caused by electrons with energy well below 2 MeV (several KeV to 300 KeV) and due to both surface charging and internal charging; (4) that the energetic electron flux would be a parameter as good as Kp and Dst to predict anomalies on Tele-X, implying that the majority of the anomalies on Tele-X were caused by electrons with energy above 2 MeV and due to internal charging. From the developed neural network models we find that for Meteosat-3 Kp, Dst, and the energetic electron flux give the total prediction rate (for anomalies and non-anomalies) of 79%, 73%, and 62%, respectively. For Tele-X the total prediction rates are 64%, 66%, and 67% from Kp, Dst and energetic electron flux, respectively. The prediction results are in agreement with the superposed epoch analysis. The neural network models developed in this study can be used to predict times with higher risks for anomalies in real-time from ACE solar wind data.

1. INTRODUCTION

The space environment (including atmosphere, plasma, radiation, and micrometeoroid/orbital debris) can adversely affect spacecraft in space. The type of space environment effects depends on the altitude and inclination of a spacecraft orbit. The magnitude of interactions between the space environment and spacecraft varies with local time, season, geomagnetic and solar activity, with magnitude varying from negligible to mission threatening.

In space plasma environment, because electron flux is dominant in the Earth's ionosphere and magnetosphere, spacecraft can be charged negatively to high electrical potential until reaching the floating potential. The charging which leads to a common potential of a spacecraft is not a problem in itself. However, the differences in surface conductivity, conductors and dielectrics will charge to different potentials in a plasma environment. This differential charging may lead to arc discharging between surfaces if the potential difference is big enough. The arc discharging could cause permanent damage to spacecraft subsystems and electromagnetic interference with sensitive electronics [*Tribble*, 1995]. Further, charging currents arise not only from the ambient plasma itself but from photoelectron and secondary electron emission. In geosynchronous orbit the currents of photoelectron emission and secondary electron emission are important sources of surface charging because plasma density is much lower and impact energy is higher than in low earth orbit.

In energetic radiation space environment (including energetic radiation belt particles, cosmic rays, solar protons), the total dose of radiation deposited over the life of the material and the dose rate are two most important factors responsible for radiation damage. Energetic electrons ($\geq$ 100 KeV) are not confined to interact with spacecraft surfaces and will penetrate the surface material into a spacecraft interior and deposit their energy. The amount of energy deposited in a material depends on the type of radiation and its energy as well as the material susceptibility. This will determine the time scale of the internal buildup of charges (internal and deep dielectric charging) for a hazardous electrostatic discharging (dielectric breakdown, gaseous arc discharge) to occur. The time scale may vary from many hours to several days [*Vampola*, 1994]. Cosmic rays and energetic solar protons can trigger single event effects (e.g., upsets, latchup) on spacecraft [*Wrenn*, 1995].

During geomagnetic quiet times, geosynchronous satellites traverse the plasmasphere and are generally earthward of the plasma sheet, and the cold plasma sphere does not support charging. During a typical substorm, a geosynchronous satellite will pass by the inner edge of the plasma sheet and observe the injection of ring current plasma, surface charging can therefore be enhanced due to the injection of hot plasma. During extended intervals of geomagnetic activity and major magnetic storms, high energetic electron fluxes develop on the outer magnetosphere, geosynchronous satellites are generally immersed in the energetic electron environment. These penetrating electrons can become embedded within dielectrics on satellites building up electric potentials over time which can exceed the breakdown potential of the dielectric [*Vampola*, 1987].

Geomagnetic storms affect spacecraft through enhanced electron fluxes. Energetic electron flux at the geosynchronous orbit is extremely dynamic, with variation of several orders of magnitude during a few days. Regarding how energetic electron flux depends on geomagnetic activity, it was shown by *Nagai* [1988] and *Koons and Gorney* [1991] that the enhancement of electron flux can extend from 1 to 5 days following the storm onset (as measured by Dst and Kp).

With new sensitive electronic components and low-mass constraints (less shielding) the influence on satellites by space weather will increase. It will be more important to predict times with higher risk for anomalies in the future. In this study, we investigate how space weather (characterised by energetic electron flux (> 2 MeV) and geomagnetic activity indices Kp and Dst) affects the two geostationary satellites, ESA Meteosat-3 and Swedish Tele-X. First we construct a space environment database for the study of 900 anomalies and 560 non-anomalies on the two satellites. Second we make the superposed epoch analysis on the database. Third we develop neural network models to predict spacecraft anomalies 1 day ahead.

2. DATA

2.1. Anomalies on Meteosat-3 and Tele-X

On Meteosat-3, an ESA meteorological satellite operating from June 1988 to November 1995, 724 anomalies were recorded from 21 June 1988 to 20 October 1995. From 2 April 1989 to 26 October 1996, 192 anomalies were recorded on Tele-X, which is a Swedish telecommunication satellite operating from April 1989 to January 1998.

Occurrence of the anomalies on Meteosat-3 and Tele-X is displayed in Figure 1(d). The local time dependence of the anomalies on Meteosat-3 and Tele-X was shown in [*Andersson et al.*, 1997], with more anomalies occurred in the sector between local midnight and 9:00 am. This is because electrons and ions subject to gradient and curvature shifts are deflected by the geomagnetic field in different directions, spacecraft orbiting during this time sector will be exposed to an abundance of electron with higher energy (KeV or higher) during increasing geomagnetic activity (substorms or storms). Spacecraft orbiting between 6:00

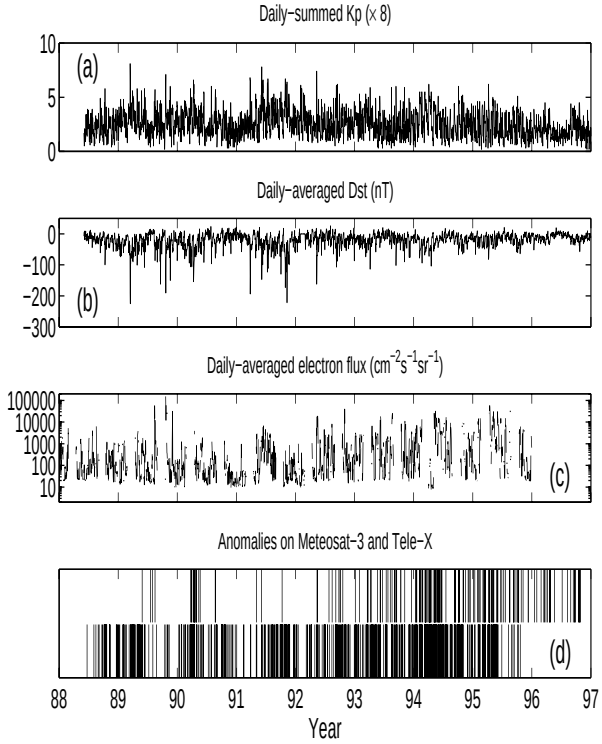

Figure 1. Anomalies on Meteosat-3 and Tele-X during 880621-961020 and the corresponding space environment conditions. (a) Daily-summed Kp; (b) Daily-averaged Dst (nT); (c) Daily-averaged energetic electron flux with energy above 2 MeV ($cm^{-2}s^{-1}sr^{-1}$), inferred from GOES-7 measurements; and (d) Anomalies on Meteosat-3 (shown in the lower part) and on Tele-X (shown in the upper part).

pm and midnight do not experience a similar effect as it is much easier for the ambient electrons to cancel the flux of storm ions. The greatest concern during geomagnetic storms is therefore for spacecraft operating between local midnight and morning time. The semiannual variation of geomagnetic activity [*Russel and McPherron*, 1973] also has its signature in the occurrence of anomalies on Meteosat-3 and Tele-X which peaked at the equinoxes [*Andersson et al.*, 1997]. We therefore consider all the anomalies on Meteosat-3 and Tele-X equivalently as induced by space environmental factors in this study.

2.2. Space Environment Data

A variety of indices have been utilized to characterize geomagnetic activity. Some of them are designed to characterize specific aspects of the total disturbance field, while others are meant to be global, offering a measure of the worldwide level of magnetic disturbances [*Mayaud*, 1980; *Joselyn*, 1995]. The 3-hourly K index is quasi-logarithmic number between 0 and 9 by measuring the largest excursion of magnetic field strength on all three magnetometer orthogonal elements. To remove local influences, the local K index inferred from 11 observatories at geomagnetic latitudes between 45° and 63° in both northern and southern hemisphere are combined to produce a relatively global index, Kp [*Bartels*, 1949]. At these middle latitudes the observed geomagnetic

variations are not the predominant influence of only one current system and may have contributions from different magnetospheric current systems. Therefore Kp derived from geomagnetic perturbations at those latitude gives a fairly global characterisation of the energy input into the magnetosphere [*Menvielle and Berthelier*, 1991].

The Dst index, originally devised by *Sugiura* [1964], is calculated hourly from the H component recorded at 4 low latitudes magnetic observatories ($20° - 30°$ away from the dipole equator and equally spaced in longitude), where both auroral- and equatorial-electrojet effects are minimal. Dst provides a measure of the strength of the ring current (the total energy of ring current particles) and serves as an indicator of the intensity and duration of magnetic storms. Ring current is formed by ions (mainly protons and oxygen ions) and electrons in the 10-300 KeV range, where electrons do not contribute much to the ring current energy, but to penetrating radiation. Dst is essentially the value of the ring current field at the dipole equator, with some uncertainties due to magnetic contributions from other sources, e.g, magnetopause currents, asymmetric ring current, and substorm current wedge, as discussed by *Rostoker* [1972].

Kp and Dst indices and energetic electron flux (>2 MeV) are used here as environmental parameters to correlate with spacecraft anomalies. Hourly Dst and 3-hourly Kp data are taken from NSSDC OMNIWeb. Daily-averaged Dst and daily-summed Kp are actually used in this study. The daily-averaged energetic electron flux are inferred from original 5-minute averaged data measured by NOAA GOES-6, GOES-7, and GOES-8. For Kp, we take the daily-summed values since 3-hourly Kp cannot be averaged due to its quasi-logarithmic scale. The choice with daily resolution is mainly due to the fact that Meteosat-3, Tele-X and the GOES satellites are located at different longitudes along the geostationary orbit. The environment data used to study the anomalies on Meteosat-3 and Tele-X are shown in Figures 1(a)-1(c).

The data interval for an anomaly is defined as a period of time preceding a day when an anomaly occurred on Meteosat-3 or on Tele-X. The maximal interval selected is 10 days. The data interval for a non-anomaly is defined as a period of time preceding a day when anomalies did not occur on Meteosat-3 or on Tele-X and during the data interval anomalies did not occur on Meteosat-3 or on Tele-X. The maximal interval selected is 10 days as well. Therefore, definitions of an anomaly interval and a non-anomaly interval are satellite-dependent. After data processing (mainly due to the gaps in GOES measurements), we thus obtain 613 data anomaly intervals for Meteosat-3 and 167 anomaly intervals for Tele-X. We obtain 420 data non-anomaly intervals for Meteosat-3 and 140 non-anomaly data intervals for Tele-X.

3. SUPERPOSED EPOCH ANALYSIS

The superposed epoch analysis is made on the database constructed above. The results are shown in Figures 2(a)-2(c) for Meteosat-3 and Tele-X. As seen from the averaged anomaly interval pattern of Kp or Dst, anomalies tend to occur during the period of time when geomagnetic activity starts decreasing after reaching the maximum. We find the same result for anomalies on both Meteosat-3 and Tele-X. This indicates that the spacecraft anomalies frequently occurred during the recovery phase of geomagnetic storms. Furthermore, the space environment conditions during the last 4-6 days preceding an anomaly are seen to contribute statistically the most to the occurrence of anomalies on both Meteosat-3 and Tele-X. Those results are consistent with the fact that geomagnetic storms affect spacecraft through enhanced electron fluxes (with a delay from 1 to 5 days following the storm onset). The main phase generally lasts about 1 day, electron fluxes are therefore enhanced during the recovery phase of magnetic storms.

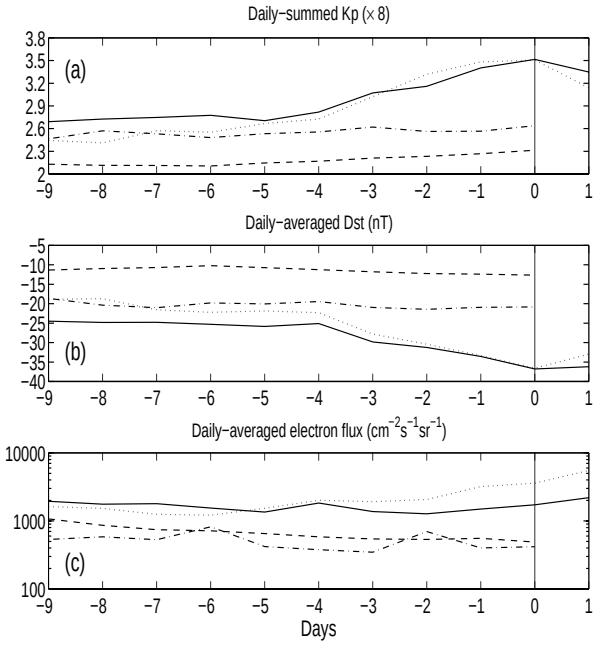

Figure 2. Superposed epoch analysis on anomaly and non-anomaly data intervals characterised by space environment parameters: (a) Daily-summed Kp; (b) Daily-averaged Dst (nT); and (c) Daily-averaged energetic electron flux with energy above 2 MeV ($cm^{-2}s^{-1}sr^{-1}$). The solid line represents the mean distribution of anomaly intervals averaged for 691 anomalies on Meteosat-3 and the dashed line represents the mean distribution of non-anomaly intervals averaged for 420 non-anomalies on Meteosat-3. The dotted line refers to the mean distribution of anomaly intervals averaged for 167 anomalies on Tele-X and the dashed-dotted line to the mean distribution of non-anomaly intervals averaged for 140 non-anomalies on Tele-X.

As seen from Figure 2, for Meteosat-3 the patterns of Kp or Dst for the averaged data interval of anomalies and non-anomalies are more clearly distinguished from each other than energetic electron flux (> 2 MeV). This means that Kp and Dst would be better input parameters than the energetic electron flux in predicting anomalies on Meteosat-3. We therefore argue that the anomalies on Meteosat-3 were mainly caused by electrons with energy well below 2 MeV and associated with both surface charging and internal charging.

In contrast, for Tele-X the averaged anomaly inter-

val and the averaged non-anomaly interval for energetic electron fluxes are also clearly distinguished from each other as those for Dst and Kp. This means that the energetic electron flux would be a parameter as good as Kp and Dst in predicting anomalies on Tele-X, thereby suggesting that the majority of the anomalies on Tele-X were caused by electrons with energy above 2 MeV and namely due to internal charging.

Susceptibility of the two satellites to the space environment conditions can be further qualitatively examined from Figure 2. In the averaged non-anomaly interval, geomagnetic activity as measured by Kp and Dst is stronger for Tele-X than for Meteosat-3. This implies that Meteosat-3 is more susceptible to increasing geomagnetic disturbances than Tele-X and that Kp and Dst would hence give more accurate prediction of anomalies on Meteosat-3 than on Tele-X.

In the averaged non-anomaly interval, the energetic electron environment of Meteosat-3 is similar to that of Tele-X. However, in the averaged anomaly interval, the energetic electron flux on Tele-X is higher than on Meteosat-3 during the last 4-5 days preceding the occurrence of anomalies. Hence, the anomalies on Tele-X is more possibly caused by energetic electron environment ($>$ 2 MeV) than those on Meteosat-3.

4. NEURAL NETWORK PREDICTIONS OF SPACECRAFT ANOMALIES

Neural networks (NNs) have been successfully applied in study of solar wind-magnetosphere coupling [*Wu and Lundstedt*, 1996, 1997a, 1997b]. With WIND solar wind plasma and interplanetary magnetic field data as input, the validity of developed NN models has further been verified from their capability to accurately predict a major magnetic storm triggered by the 1997 January halo-CME [*Wu et al.*, 1998a]. The resulting enhancement of relativistic electron fluxes in the magnetosphere was suspected as the killer of AT&T Telestar 401 satellite on January 11, 1997. NNs have also been exploited in spacecraft anomaly analysis and predictions [*Lópea and Hilgers*, 1997; *Wu et al.*, 1998b].

On the basis of the above superposed epoch analysis, we further develop NN models to predict spacecraft anomalies 1 day ahead from the space environment database. Time-delay NNs with standard gradient descent algorithm and adaptive learning scheme [*Hertz et al.*, 1991] are exploited in this paper. A time-delay NN is a supervised learning feed-forward back-propagation network with a time delay line in the input layer.

NNs are trained only on Meteosat-3 and the trained neural network models are generalised on Meteosat-3 and Tele-X. The network output is set to 1 for an anomaly and to 0 for a non-anomaly in the training set. For test, if the output is in the range (0.5,1.5), then it is classified as an anomaly; If the output is in the range (-0.5,0.5), it is classified as a non-anomaly; If the output falls outside the 2 ranges, then the output is classified as uncertain.

4.1. Training and test data

Daily averaged energetic electron flux, daily averaged Dst and daily sum of Kp are the input parameter. The data of Dst, Kp and the logarithm of electron flux are linearly normalised to [-1, 1]. The maximum and minimum values of the daily sum of Kp are 8.1 ($\times$ 8) and 0.2 ($\times$ 8). The maximum and minimum values of the daily Dst are 2.6 nT and -225.0 nT. The maximum and minimum values of the daily electron flux are 2.88×10^5 and 1.00 ($cm^{-2}s^{-1}sr^{-1}$).

Training takes place on 70% of the events (including anomalies and non-anomalies) on Meteosat-3 only. Trained NNs are first generalised from the rest 30% of the events on Meteosat-3 (test set #1) and then tested on Tele-X (test set #2) to see how the trained NN models can generalise from Meteosat-3 to Tele-X. The training set consists of 454 anomalies and 279 non-anomalies on Meteosat-3. The test set #1 consists of 159 anomalies and 131 non-anomalies on Meteosat-3. The test set #2 consists of 167 anomalies and 140 non-anomalies on Tele-X.

4.2. Anomaly predictions

For each time delay line in the network input layer, different number of the network hidden neurons is used to find the optimal network models. We summarize the best prediction results in Figures 3(a)-3(c) for the input of Kp, Dst, and energetic electron flux. The prediction rate for anomalies is defined as the number of correct predictions for anomalies divided by the number of anomalies in a dataset. The prediction rate for non-anomalies is defined as the number of correct predictions for non-anomalies divided by the number of non-anomalies in the dataset. The total prediction rate is defined as the total number of correct predictions for both anomalies and non-anomalies divided by the total number of anomalies and non-anomalies in the dataset.

For Meteosat-3, we find that Kp gives the best prediction for anomalies and non-anomalies on Meteosat-3 at $\tau = 8$ (τ is the length of the time delay line in days), with the total prediction rate 79%, the prediction rate for anomalies 78% and the prediction rate for non-anomalies 80%. The corresponding total prediction rate is 64% for Tele-X, the prediction rate is 78% for anomalies and is 46% for non-anomalies.

With Dst as input, the best total prediction rate is 73% for Meteosat-3 at $\tau = 8$, the prediction rate is 75% for anomalies and is 72% for non-anomalies. The corresponding total prediction rate is 64% for Tele-X, the prediction rate is 81% for anomalies and is 44% for non-anomalies.

With electron flux as input, the best total prediction rate is 66% for Meteosat-3 at $\tau = 2$, the prediction rate for anomalies is 90% and for non-anomalies is 38%. The corresponding total prediction rate is 66% for Tele-X, the prediction rate is 90% for anomalies and is 36% for non-anomalies.

For Meteosat-3, Kp gives slightly better predictions than Dst, whereas energetic electron flux gives prediction rates some 10% less than Kp and Dst. This is

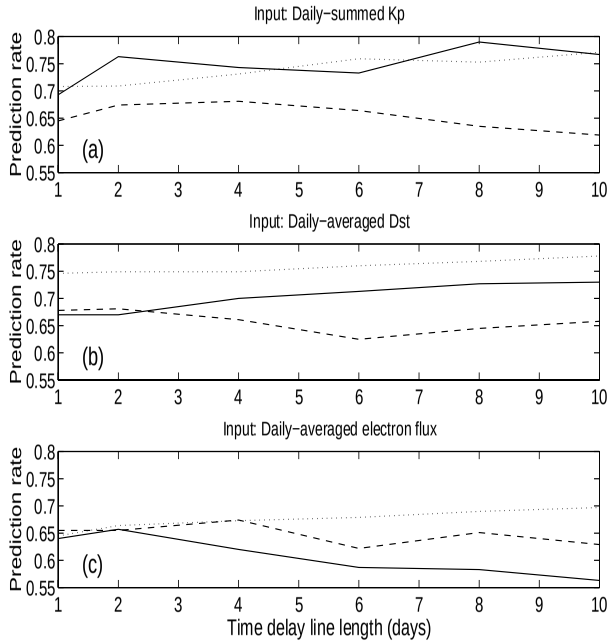

Figure 3. The total prediction rate for both anomalies and non-anomalies versus the length of the time delay line in the network input layer, with the input parameter: (a) Daily-summed Kp; (b) Daily-averaged Dst (nT); and (c) Daily-averaged energetic electron flux with energy above 2 MeV ($cm^{-2}s^{-1}sr^{-1}$). The solid line stands for the total prediction rate on Meteosat-3, the dashed line for the total prediction rate on Tele-X, and the dotted line for the prediction rate for training on the events on Meteosat-3.

in agreement with the results from the above superposed epoch analysis. As described in section 2.2, Kp includes contributions both from substorms currents and the ring current, thereby giving a fairly global characterisation of the energy input into the magnetosphere. And Dst has contributions mainly from the equatorial ring current, serving as an indicator of the storm intensity. Since Kp is a more global measure of geomagnetic activity, including contributions from both substorms and storms, than Dst, Kp would give better predictions than Dst.

During increasing geomagnetic activity, electron fluxes with low and high energy are enhanced which are responsible for spacecraft surface charging and internal dielectric charging, respectively. As inferred from the above analysis, surface charging and internal charging both could have caused the anomalies on Meteosat-3. Thus, both Kp and Dst should give more accurate prediction than the energetic electron flux (only responsible for internal charging). Because ring current ions and electrons are in the energy range 10-300 KeV and energy of injected electrons by substorms are of KeV order, more accurate prediction from Kp and Dst may indicate that most of the anomalies on Meteosat-3 were caused by electrons in energy range from several KeV up to 300 KeV.

For Tele-X we find that energetic electron flux gives slightly higher prediction rate for Tele-X than for Meteosat-3 and that the prediction rates from Kp and Dst are higher for Meteosat than for Tele-X. In addition, the energetic electron flux, Kp, and Dst produce almost the same prediction rate for Tele-X. These are in agreement with the analysis in section 3 in terms of the type of the anomalies on the two satellites and the resultant prediction accuracy.

However, while making post-error analysis we should be aware of a number of the following factors: (1) Definition of anomaly and non-anomaly is satellite-dependent; (2) The training was only on Meteosat-3; and (3) The local conditions (e.g. design, material) on Tele-X are different from Meteosat-3 (Local environment conditions along the geostationary orbit have been averaged out due to the daily input data).

The first 2 factors did introduce the error in the prediction rate. Some anomalies on Meteosat-3 which also occurred on Tele-X on the same day were included in the training set, since we consider only one satellite at a time regardless what happened to the other. Thus while testing the trained NN model on Tele-X, the prediction rate must be higher for the anomalies in the test set because some of them have been included in the training set. On the contrary, the prediction rate must be lower for the non-anomalies on Tele-X because some of the non-anomaly intervals on Tele-X overlap the part of anomaly intervals on Meteosat-3 which have also been included in the training set as anomaly intervals. The purpose to define anomalies and non-anomalies satellite-dependent is to see how the models trained on one satellite can generalise to the other.

The error introduced by the last factor results from the difference of the susceptibility of the 2 satellites to the space environment, which has been examined in section 3. The types and number of anomalies induced by space environment are closely related to the satellite susceptibility. The susceptibility might be reflected by the threshold value which enables to give an equal prediction rate for anomalies and for non-anomalies on Tele-X, as shown by *Wu et al.* [1998b].

As seen from the generalisation performance shown in Figure 3, for Meteosat-3 the prediction rate is relatively stable from the input Kp or Dst as $\tau \geq 4$. Given by the energetic electron flux the prediction rate decreases as $\tau > 2$. For Tele-X the prediction rate peaks at $\tau = 4$ for the input of Kp and of the energetic electron flux, while $\tau = 2$ gives the best prediction rate from the input Dst. Thus, the time scale of accumulation effects to cause the anomalies on the two satellites may be in the range 2-4 days.

We also use different combinations of Dst, Kp and energetic electron flux as the input parameters. However, the predictions are not distinctively improved. This could be because the essential input dimension does not increase due to strong correlations among the three parameters [*Koons and Gorney*, 1991].

The developed NN models here can be used to predict times with higher risks for anomalies in real-time from ACE solar wind data because the NN models which can accurately predict Dst from solar wind data have been available [*Wu and Lundstedt*, 1996, 1997a, 1997b; *Wu et al.*, 1998a].

5. SUMMARY AND CONCLUSIONS

In this paper we investigate how space weather affects geostationary spacecraft through superposed epoch analysis and develop NN models to predict anomalies on Meteosat-3 and Tele-X one day in advance. The main results are summarised below.

We find from the superposed epoch analysis that

- The spacecraft anomalies frequently occurred during the recovery phase of geomagnetic storm;
- The space environment conditions during the last 4-6 days preceding an anomaly contribute statistically the most to the anomaly occurrence;
- Kp and Dst are better parameters than the energetic electron flux to predict anomalies on Meteosat-3, implying that the anomalies on Meteosat-3 were largely caused by electrons with energy well below 2 MeV (several KeV to 300 KeV) and due to both surface charging and internal charging;
- The energetic electron flux would be a parameter as good as Kp and Dst to predict anomalies on Tele-X, implying that the majority of the anomalies on Tele-X were caused by electrons with energy above 2 MeV and due to internal charging.

We find from network predictions that for Meteosat-3 daily-summed Kp, daily-averaged Dst, and daily-averaged energetic electron flux give the total prediction rate of 79%, 73%, and 62%, respectively. For Tele-X, Kp, Dst and energetic electron flux gives the total prediction rate of 64%, 66%, and 67%, respectively. The prediction results are consistent with the superposed epoch analysis.

The developed NN models can be used to predict times with higher risks for anomalies in real-time from ACE solar wind data.

Finally we have the following suggestions for the future work:

- Analyse and model on higher time resolution, therefore the local space environment conditions can be taken into account;
- Use other global geomagnetic indices like am or Km and substorm indices (e.g., AE);
- Use low energy electron flux to capture the anomalies caused by surface charging, in combination with energetic electron flux.

REFERENCES

Andersson, L., O. Norberg, L. Eliasson, J.-G. Wu, H. Lundstedt, and P. Wintoft, Prediction of Anomalies on Geostationary Satellites, in ESA WPP-148 Proceedings of Second International Workshop on AI Applications in Solar-Terrestrial Physics, edited by Ingrid Sandahl and Eivor Jonsson, pp. 213-218, 1997.

Bartels, J., The standardised index, Ks, and the planetary index, Kp, IATME Bull. 12b, 97, IUGG Pub. Office, Paris, 1949.

Hertz, J., A. Krogh and R. G. Palmer, *Introduction to the Theory of Neural Computation*, ch. 6, Addison-Wesley, 1991.

Joselyn, J.A., Geomagnetic activity forecasting: The state of the art, *Rev. of Geophys.*, 33 (3), 383, 1995.

Koons, H.C., and D.J. Gorney, A Neural Network Model of the Relativistic Electron Flux at Geosynchronous Orbit, *J. Geophys. Res.*, 96, 5549, 1991.

López Honrubia, F.J., A. Hilgers, Some Correlation Techniques for Environmentally Induced Spacecraft Anomalies Analysis, *J. Spacecraft and Rockets*, 34, 670, 1997.

Mayaud, P.N., (eds.), *Derivation, Meaning, and Use of Geomagnetic Indices, Geophys. Monogr. Ser.,* vol. 22, AGU, Washington, D.C., 1980.

Menvielle, M., and A. Berthelier, The K-derived planetary indices: Description and availability, *Rev. Geophys.*, 29, 415, 1991.

Nagai, T., Space Weather Forecast: Prediction of Relativistic Electron Intensity at Geosynchronous Orbit, *Geophys. Res. Lett.*, 15, 425, 1988.

Rostoker, G., Geomagnetic indices, *Rev. Geophys. Space Phys.*, 10, 935, 1972.

Russell, C.T., and R.L. McPherron, Semiannual variation of geomagnetic activity, *J. Geophys. Res.*, 78, 92, 1973.

Tribble, A.C., *The Space Environment: Implications for Spacecraft Design*, Princeton University Press, 1995.

Sugiura, M., Hourly values of equatorial Dst for the IGY, *Ann. Int. Geophys. Year*, 35, 1964.

Vampola, A.L., Thick dielectric charging on high-altitude spacecraft, *J. Electrost.*, 20, 21, 1987.

Vampola, A.L., Analysis of Environmentally Induced Spacecraft Anomalies, *J. Spacecraft and Rockets*, 31, 154, 1994.

Wrenn, G.L., Conclusive Evidence for Internal Dielectric Charging Anomalies on Geosynchronous Communications Spacecraft, *J. Spacecraft and Rockets*, 32, 514, 1995.

Wu, J.-G., and H. Lundstedt, Prediction of geomagnetic storms from solar wind data using Elman recurrent neural networks, *Geophys. Res. Lett.*, 319, 1996.

Wu, J.-G., and H. Lundstedt, Geomagnetic storm forecast from solar wind data with the use of dynamic neural networks, *J. Geophys. Res.*, 102, 14255-14268, 1997a.

Wu, J.-G., and H. Lundstedt, Neural network modeling of solar wind-magnetosphere interaction, *J. Geophys. Res.*, 102, 14457-14466, 1997b.

Wu, J.-G., H. Lundstedt, P. Wintoft, and T.R. Detman, Neural network models predicting the magnetospheric response to the 1997 January halo-CME event, *Geophys. Res. Lett*, 25, 3031-3034, 1998a.

Wu, J.-G., H. Lundstedt, L. Andersson, L. Eliasson, and O. Nordberg, Study of plasma and energetic electron environment and effects, Technical note Work package 220, ESTEC/Contract No. 11974/96/NL/JG(SC), 1998b.